Critical behavior of a one-dimensional fixed-energy stochastic sandpile

Ronald Dickman,[1] Mikko Alava,[2] Miguel A. Muñoz,[3] Jarkko Peltola,[2] Alessandro Vespignani,[4] and Stefano Zapperi[5]

[1]*Departamento de Física, ICEx, Universidade Federal de Minas Gerais, Caixa Postal 702, 30161-970 Belo Horizonte, Minas Gerais, Brazil*

[2]*Laboratory of Physics, Helsinki University of Technology, Helsinki, HUT-02105, Finland*

[3]*Institute Carlos I for Theoretical and Computational Physics and Departamento de Electromagnetismo y Física de la Materia, 18071 Granada, Spain*

[4]*The Abdus Salam International Centre for Theoretical Physics (ICTP), P.O. Box 586, 34100 Trieste, Italy*

[5]*INFM, Dipartimento di Fisica, Enrico Fermi, Università de Roma ''La Sapienza,'' Piazzale Aldo Moro 2, 00185 Roma, Italy*

We study a one-dimensional fixed-energy version (that is, with no input or loss of particles) of Manna's stochastic sandpile model. The system has a continuous transition to an absorbing state at a critical value of the particle density, and exhibits the hallmarks of an absorbing-state phase transition, including finite-size scaling. Critical exponents are obtained from extensive simulations, which treat stationary and transient properties, and an associated interface representation. These exponents characterize the universality class of an absorbing-state phase transition with a static conserved density in one dimension; they differ from those expected at a linear-interface depinning transition in a medium with point disorder, and from those of directed percolation.

I. INTRODUCTION

Sandpile models are the prime example of self-organized criticality (SOC) or scale invariance in the apparent absence of tuning parameters [1–4]. SOC in a slowly driven sandpile is associated with an absorbing-state phase transition in the corresponding nondriven or fixed-energy sandpile (FES) [3–8]. While most studies of sandpiles have probed the slow-driving limit (addition and loss of sand grains at an infinitesimal rate), there is great interest in understanding the scaling properties of FES models as well [7,9–11]. In this paper we present extensive numerical results on scaling properties, and the dynamics of an interface representation, of a particularly simple one-dimensional FES. For background on FES models in the context of absorbing-state phase transitions we refer the reader to Ref. [12]; Ref. [13] discusses the relation of sandpiles to driven interface models.

A central feature of sandpile models is the presence of a conserved field, the density of particles. This field couples to the activity density, which is the order parameter. When, as in the case of FES, the conserved field is frozen in the absence of activity, the critical behavior is expected to fall in a universality class distinct from that of directed percolation [14]. [Directed percolation (DP) universality is generic for continuous absorbing-state transitions in the absence of a conservation law.] One motivation for the present study is to determine the critical behavior of a one-dimensional example of this recently identified class.

In sandpiles the configuration evolves through a series of ''toppling'' events, which may be either deterministic or stochastic. The well-known Bak-Tang-Wiesenfeld (BTW) sandpile has a deterministic toppling rule, allowing many stationary-state properties of the driven sandpile to be found exactly [15,16]. A less desirable aspect of the deterministic dynamics is that in the steady-state only a small subset of the possible configurations (determined by the initial state) are visited [15]. This leads to strong nonergodic effects in the

FES version of the BTW automaton [12]. Here we study a stochastic FES that is expected to be ergodic.

We find that the model exhibits the hallmarks of an absorbing-state critical point, including finite-size scaling, familiar from studies of directed percolation or the contact process [17]. The one-dimensional Manna model defines a universality class different from that of DP, and that of the linear-interface depinning transition model (LIM) [18]. Connections have been drawn between sandpile criticality and both DP (in a field-theoretical description [19]) and the LIM (via an interface mapping [12,13]). The balance of this paper is organized as follows. In Sec. II we define the model and our simulation procedure. Numerical results are analyzed, in the contexts of absorbing-state phase transitions and of driven interfaces, in Sec. III. In Sec. IV we summarize and discuss our findings.

II. MODEL

Our model, a variant of the Manna sandpile [20,21], is defined on a one-dimensional lattice of L sites with periodic boundaries. The configuration is specified by the number of particles $z_i = 0,1,2,\ldots$ at each site; sites with $z_i \geq 2$ are said to be *active*. A Markovian dynamics is defined by the toppling rate, which is unity for all active sites and zero for sites with $z_i < 2$. When a site i topples, it sends two particles to adjacent sites ($z_i \rightarrow z_i - 2$); the particles move independently to randomly chosen nearest neighbors j and j' ($j,j' \in \{i+1,i-1\}$). (Thus $j = j'$ with probability 1/2.) The dynamics conserves the number of particles N, which is fixed by the initial configuration.

For densities $\zeta = N/L \leq 1$ absorbing configurations exist, in which all sites have $z_i < 2$. But since the fraction of absorbing configurations vanishes as $\zeta \rightarrow 1$, it is reasonable to expect a phase transition from an absorbing to an active phase at some $\zeta_c < 1$. Simulations bear this out and show that there is a continuous transition at $\zeta_c \simeq 0.9488$.
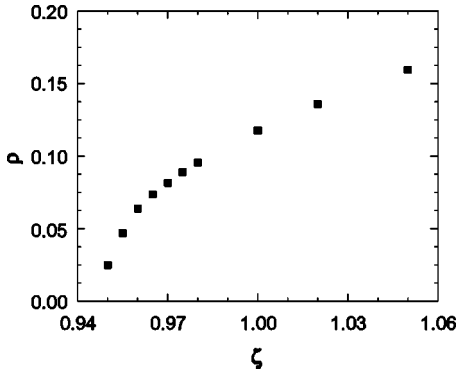
FIG. 1. Stationary active-site density versus energy density ζ. The points represent extrapolations of data for $L = 100$–5000 to the $L \rightarrow \infty$ limit.

In most cases we use random sequential dynamics: the next site to topple is chosen at random from a list of active sites, which is updated following each toppling. The time increment associated with a toppling is $\Delta t = 1/N_A$, where N_A is the number of active sites just prior to the event. In this way $\langle N_A \rangle$ sites topple per unit time, just as in a simultaneously updated version of the model. (In a simultaneous dynamics all active sites topple at each update; $\Delta t \equiv 1$, regardless of the number of active sites.) We expect the two dynamics to be equivalent insofar as scaling properties are concerned; simultaneous updating was used in some of the interface representation studies discussed below.

In most of our simulations, the initial condition is generated by distributing ζL particles randomly among the L sites, yielding an initial (product) distribution that is spatially homogeneous and uncorrelated. Once the particles have been placed, the dynamics begins. (We verified that allowing some toppling events *during* the insertion phase has no effect on the stationary properties.)

III. SIMULATION RESULTS

A. Absorbing-state phase transition

We simulated the model on systems ranging from $L = 100$ to about 10^4 sites. (Since $\zeta = N/L$ with N and L integers, we are obliged to use different sets of L values to study different densities ζ.) In stationary-state simulations, we collect data over an interval of t_m time units, following a relaxation period of t_r. For small systems, t_m and t_r are of the order of 10^3, but for our largest systems we used $t_r \geq 5 \times 10^6$ and $t_m = 2.5 \times 10^6$. We verified that our results show no systematic variation with time for $t > t_r$. In practice t_m is limited because for $\zeta \simeq \zeta_c$, the survival probability decays sensibly over this time scale; in some cases only about 25% of the trials survive to time $t_r + t_m$. We average over N_s independent trials, each with a different initial configuration with N_s ranging from 2×10^5 for $L = 100$, to 500 or 1000 for $L \simeq 10^4$.

Figure 1 shows the overall dependence of the stationary active-site density as a function of ζ; the points represent extrapolations of results for $L = 100$–5000 to the $L \rightarrow \infty$ limit. The data indicate a continuous transition from an absorbing
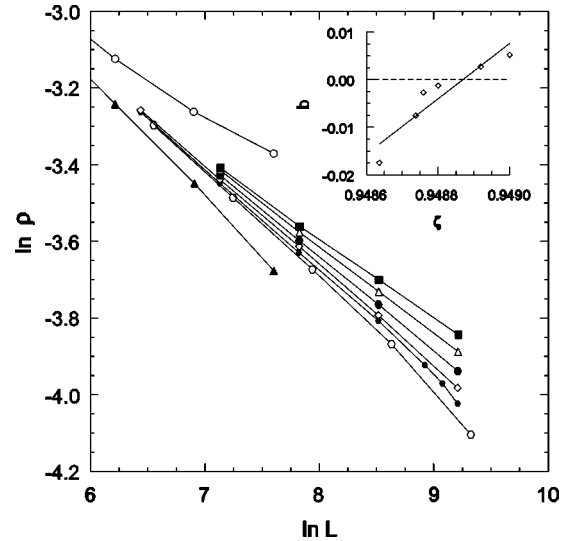

FIG. 2. Stationary active-site density vs system size. From bottom to top, ζ = 0.948, 0.948 57, 0.948 64, 0.948 74, 0.9488, 0.948 92, 0.949, and 0.95. The inset shows the curvature b of the log-log plot as a function of ζ for $L \geq 1000$. The straight line is a least-squares linear fit.

state ($\rho_a = 0$) to an active one at ζ_c in the vicinity of 0.95.

Our first task is to locate the critical value ζ_c. To this end we studied the stationary active-site density $\bar{\rho}_a$ and its second moment $\bar{\rho}_a^2$, anticipating that as in other absorbing-state phase transitions, the active-site density (i.e., the order parameter) will obey finite-size scaling [22],

$$\bar{\rho}_a(\Delta, L) = L^{-\beta/\nu_\perp} \mathcal{R}(L^{1/\nu_\perp} \Delta), \tag{1}$$

where $\Delta \equiv \zeta - \zeta_c$ and $\mathcal{R}$ is a scaling function. $\mathcal{R}(x) \sim x^\beta$ for large x, since for $L \gg \xi \sim \Delta^{-\nu_\perp}$ we expect $\bar{\rho}_a \sim \Delta^\beta$ (ξ is the correlation length). When $\Delta = 0$ we have $\bar{\rho}_a(0, L) \sim L^{-\beta/\nu_\perp}$. For $\Delta > 0$, by contrast, $\bar{\rho}_a$ approaches a stationary value, while for $\Delta < 0$ it falls off as L^{-d}. Thus in a double-logarithmic plot of $\bar{\rho}_a$ versus L, supercritical values ($\Delta > 0$) are characterized by an upward curvature, while for $\Delta < 0$ the graph curves downward (see Fig. 2). Using this criterion (specifically, zero curvature in the data for $L \geq 1000$), we find $\zeta_c = 0.948 \, 87(7)$, with the uncertainty reflecting the scatter in our numerical results for the curvature (see Fig. 2, inset). The associated exponent ratio is $\beta/\nu_\perp = 0.235(11)$. A similar analysis of the data for $\bar{\rho}_a^2$ yields $\zeta_c = 0.948 \, 83(5)$ with an exponent of $2\beta/\nu_\perp = 0.483(18)$. We therefore adopt the estimates $\zeta_c = 0.948 \, 85(7)$ and $\beta/\nu_\perp = 0.239(11)$.

In order to characterize dynamical scaling, we studied the survival probability $P(t)$, i.e., that there is at least one active site in the system. In systems with an absorbing state, the survival probability decays exponentially, $P(t) \sim e^{-t/\tau}$, with the lifetime $\tau \sim L^z$ at the critical point. Figure 3 shows the typical behavior of the survival probability in relation to the relaxation of the active-site density ρ. We see that the latter relaxes on a shorter time scale than $P(t)$, and that the survival probability does indeed decay exponentially in the sta-
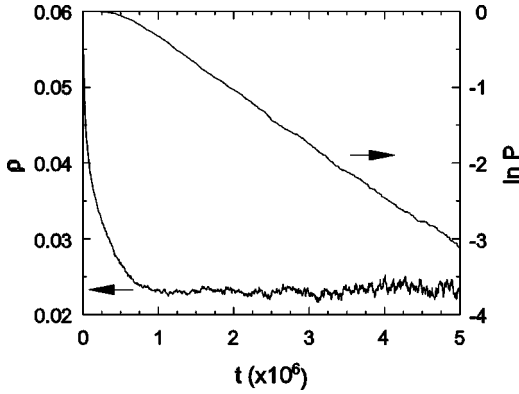
FIG. 3. Decay of the active-site density ρ and of the survival probability P in a system of $L=5012$ sites at $\zeta=0.948\,92$.

tionary regime as is usual at an absorbing-state phase transition [17]. Analyzing the lifetime in a series of studies at $\zeta = 0.9488$ for system sizes $L=1250$, 2500, 5000, and 10^4, we find $z=1.58$; a similar series of studies at $\zeta=0.948\,92$ yields $z=1.70$ (see Fig. 4). (We generated 3000–5000 realizations for each system size.) Given our estimate for ζ_c quoted above, we conclude that $z=1.63(7)$; the rather large uncertainty reflects the sensitivity of our z estimates to small changes in ζ_c. The scaling of the time τ_ρ for the active-site density to attain its stationary value yields a similar result.

We also studied the autocorrelation function for the number of active sites N_a,

$$C(t) = \frac{\langle N_a(t_0+t)N_a(t_0)\rangle - \langle N_a\rangle^2}{\langle N_a^2\rangle - \langle N_a\rangle^2} \qquad (2)$$

in the stationary state. To obtain clean results for $C(t)$ we study surviving trials in relatively long runs (from $t_m = 2\times10^5$ for $L=625$, to 5×10^6 for $L=10^4$; this obliges us to reduce our sample to 200 surviving trials for $L\leqslant2500$ and 100 surviving trials for $L\geqslant5000$). Results for $\zeta=0.9488$ are shown in Fig. 5: $C(t)$ decreases monotonically, but does not follow a simple exponential decay. To study the dependence of the relaxation time on system size, we determine the tem-
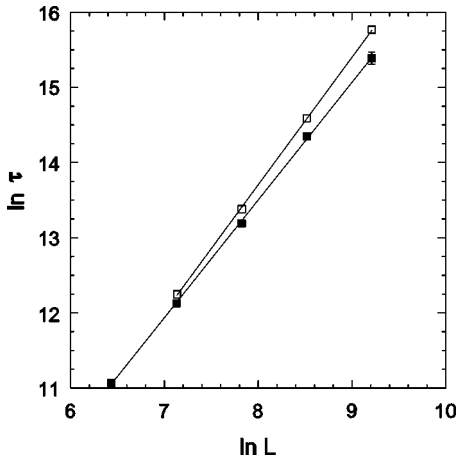

FIG. 4. Lifetime τ vs system size. Filled symbols, $\zeta=0.9488$; open, $\zeta=0.948\,92$. The straight lines are least-squares linear fits.
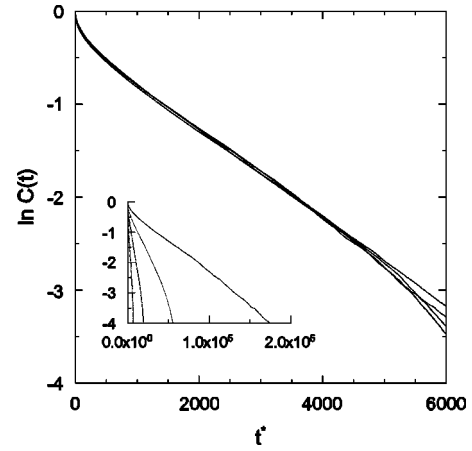

FIG. 5. Inset: Stationary autocorrelation function $C(t)$ vs t at $\zeta=0.9488$ for (left to right) $L=625$, 1250, 2500, 5000, and 10^4. In the main graph the data are plotted vs a rescaled time t^* defined in the text.

poral rescaling factor r required to obtain a data collapse between $C(t;L/2)$ and $C(t/r;L)$. A good collapse is possible (see Fig. 5), but the rescaling factor depends on L; for $L = 2^n\times625$, we use $t^*=t/r^n$ with $r=2.93$, 2.91, and 2.89 for $n=1$, 2, and 3, respectively. The rescaling factor r appears to approach a limiting ($L\to\infty$) value of 2.80(5), corresponding to a relaxation time that scales as $\tau\sim L^{\nu_\parallel/\nu_\perp}$ with $\nu_\parallel/\nu_\perp\equiv z = \ln r/\ln 2\simeq1.5$. This value is consistent with that obtained from the lifetime analysis, but is less reliable, since $C(t)$ does not follow a simple exponential decay, and we have to extrapolate the rescaling factor to $L\to\infty$.

Next we examine the stationary scaling of the order parameter away from the critical point. We determined the stationary active-site density $\bar\rho_a(\zeta,L)$ for ζ in the vicinity of ζ_c for system sizes $L=100$-5000. We analyze these data using the finite-size scaling form of Eq. (1), which implies that a plot of $L^{\beta/\nu_\perp}\bar\rho_a(\Delta,L)$ versus $L^{1/\nu_\perp}\Delta$ should exhibit a data collapse. We shift each data set (in a log-log plot of $L^{\beta/\nu_\perp}\rho_a$ versus $L^{1/\nu_\perp}\Delta$) vertically by $(\beta/\nu_\perp)\ln L$, using $\beta/\nu_\perp = 0.239$ as found above, and determine the horizontal shifts $S(L)$ required for data collapse. The latter follow $S(L) = \nu_\perp^{-1}\ln L$ with $\nu_\perp^{-1}=0.553(3)$. That these values yield an excellent data collapse is evident from Fig. 6. The slope of the scaling plot (linear regression using the 25 points with $\ln(L^{1/\nu_\perp}\Delta)>-0.5$) yields $\beta=0.410(4)$. This is somewhat smaller than, but consistent with, the estimate $\beta=0.43(2)$ obtained by combining $\nu_\perp^{-1}=0.553(3)$ and $\beta/\nu_\perp=0.239(11)$. We adopt $\beta=0.42(2)$ as our final estimate.

B. Interface representation

The interface representation is constructed by defining height variables $H_i(t)$ that count the number of topplings at site i up to time t. The dynamics of the interface representation is discussed in Refs. [12,13]; the latter reference describes the discrete interface equation for the Manna model in greater detail.

In the interface description the system undergoes a depinning transition at a critical force value equivalent to $\zeta=\zeta_c$
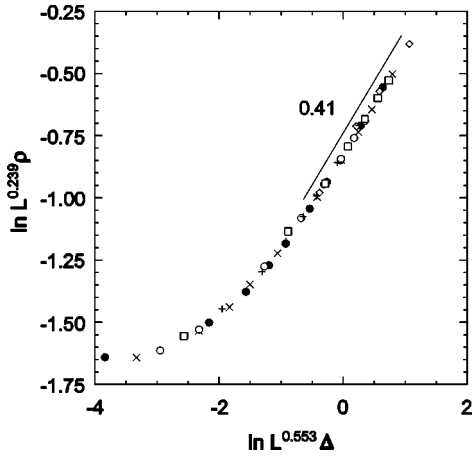
FIG. 6. Scaling plot of the active-site density versus $\Delta \equiv \zeta - \zeta_c$. Symbols: $+$, $L=100$; $\bullet$, $L=200$; $\times$, $L=500$; $\bigcirc$, $L=1000$; $\square$, $L=2000$; $\diamond$, $L=5000$.

FIG. 7. Scaling plot of $\widetilde{W}^2 \equiv W^2/L^{2\alpha}$ vs $\widetilde{t} \equiv t/L^z$ for $\zeta = 0.9489$, using $\alpha = 1.41$ and $z = 1.645$. System sizes (top to bottom) $L = 1253$, 2506, 5012, 10 024, and 20 048.

[23,24]. The interface behavior, assuming simple scaling, is described by two exponents: the roughness exponent α and the early-time exponent β_W. Introducing the width W as usual,

$$W^2(t,L) = \langle [H_i(t) - \bar{H}(t)]^2 \rangle \qquad (3)$$

[here $\bar{H}(t)$ is the mean height], these exponents are defined via

$$W^2(t,L) \sim \begin{cases} t^{2\beta_W} & t \ll t_\times \\ L^{2\alpha} & t \gg t_\times, \end{cases} \qquad (4)$$

where the crossover time $t_\times \sim L^z$. Assuming that the correlations in the interface can be described by a single length scale, we have the exponent relation $\beta_W z = \alpha$.

This scaling picture, familiar from the study of surface growth, was recently shown to apply in the case of a simple absorbing-state phase transition [25]. For the one-dimensional Manna model the situation is complicated by several factors. First, the noise appearing in the interface description has two contributions: a columnar component reflecting the initial configuration and a noise field arising from the random redistribution of particles in toppling events [13]. The interface dynamics will therefore exhibit a crossover from a regime dominated by the initial configuration to a randomness-dominated regime. This effect also appears in higher dimensions, but in $d=1$, due to the meager phase space, relaxation is much slower and transient effects may be much more severe.

A special aspect of one-dimensional interface models is anomalous scaling, i.e., the two-point correlation function of the surface roughness scales with a different exponent, α_{loc}, than the exponent α defined in Eq. (4). For fundamental reasons, $\alpha_{loc} \leq 1$ [18,26]. The exponent α can attain larger values; for example, $\alpha = 1.25$ for the one-dimensional LIM [18]. The exponents are related via $\alpha = \alpha_{loc} + \kappa$, where κ measures the divergence of the height difference between neighboring sites with time. Thus, anomalous scaling implies that the typical height difference between neighboring sites
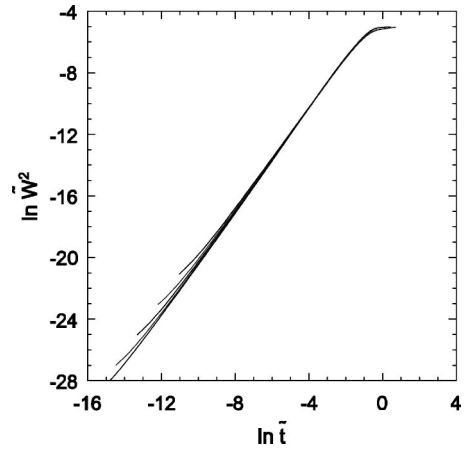
increases without limit as $t \to \infty$. Since larger systems have a longer lifetime, this has implications for the roughness as measured by $W^2_{sat} = W^2(\tau_{sat}, L)$, τ_{sat} being the time at which the absorbing state is reached. The saturation width W_{sat} scales as L^α, with α related to β_W and z as above. In models exhibiting an absorbing state such as the contact process or a FES, the width saturates only because activity eventually ceases; the width in *surviving* trials does not saturate. This is in marked contrast to interface models, in which the width saturates due to the Laplacian term representing surface tension, since the noise is bounded. The interface description of the Manna model, like other absorbing-state phase transitions and their associated interface representations [25], includes a noise term whose strength grows while there is activity [13].

Finally, in absorbing-state models, interface scaling appears to be strongly linked to the approach to the stationary state. In a model with simple scaling (i.e., unique diverging length and time scales and no conserved quantities), the growth exponent β_W is related to the critical exponent θ governing the initial decay of activity via $\beta_W + \theta = 1$ [25]. In the present case relaxation is complicated by effects that may mimic (for a certain time) columnar disorder.

We studied the interface width $W^2(t,L)$ in systems of size $L = 1253$, 2506, 5012, 10 024, and 20 048, at $\zeta = 0.948\,92$. The dependence of the saturation width on system size yields $\alpha = 1.42(1)$. We then attempt to collapse the data for $W^2(t,L)$ using this exponent and varying z to obtain the best collapse; in this way we find $z = 1.65(2)$. The resulting scaling plot (Fig. 7) of $\widetilde{W}^2 \equiv W^2/L^{2\alpha}$ versus $\widetilde{t} \equiv t/L^z$ shows a good collapse, and an apparent power-law growth in the roughness, following an initial transient. From the scaling relation $\beta_W = \alpha/z$ we obtain $\beta_W = 0.863(13)$; a direct fit to the time-dependent width data yields $\beta_W = 0.87(2)$. For comparison, an independent series of studies at $\zeta = 0.9490$ were performed to determine τ_{sat} and the saturation width W_{sat} for $L = 400$ to $L = 6400$. Power-law fits to these data yield essentially consistent results, i.e., $\alpha = 1.48(2)$,
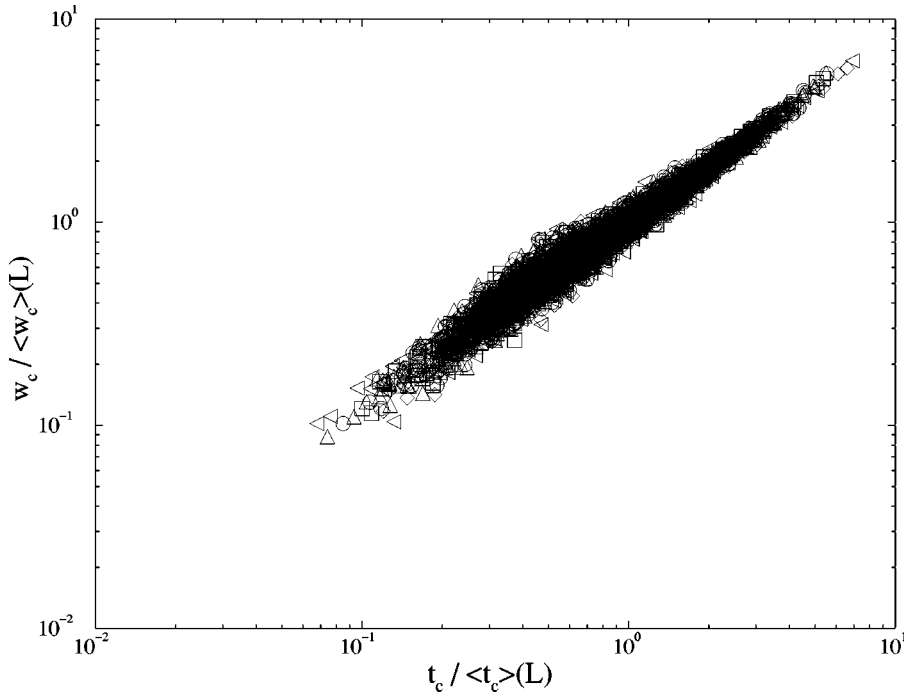
FIG. 8. Scaling plot of saturation width vs lifetime in individual trials, $\zeta = 0.9490$, $L = 400$–6400.

$\beta_W = 0.86(2)$, and $z = 1.70(3)$. Figure 8 shows a clear power-law dependence of the saturation width on the lifetime in *individual runs*.

Similarly to the case of the LIM [18], we find that there is an independent *local* roughness exponent α_{loc} that describes the two-point kth order height-height correlation function $G_k(r) = \langle |H_{i+r} - H_i|^k \rangle \sim r^{k\alpha_{loc}}$ for $r < \xi(t) \sim t^{1/z}$. We find $\alpha_{loc} = 0.59(3)$ for $k = 1, \ldots, 8$. This shows that the interface is self-affine, not multifractal.

We note that the interface exponents of the Manna sandpile are *not* those of the one-dimensional LIM. This is most likely due to the fact that, perhaps differently from the two- and higher-dimensional cases, here it is important that the noise term *increases* in strength with the propagation of the interface, or with sustained activity. Thus the anomaly exponent κ indicates an even stronger dependence of the step height on L at saturation than in the LIM. The same is also true if the step height is considered as a function of time for $t < \tau_{sat}$: we find $\kappa_{Manna} \sim 0.82 \sim \kappa_{LIM} + 0.5$.

C. Initial relaxation

At the critical point of a simple absorbing-state model such as the contact process, starting from a uniform initial condition with activity density $\rho_a > 0$, ρ_a exhibits an initial power-law decay, $\rho_a \sim t^{-\theta}$, followed by a crossover to the quasistationary value $\bar{\rho}_a \sim L^{-\beta/\nu_\perp}$ [17]. As noted above the growth exponent is related to the activity-decay exponent via $\theta + \beta_W = 1$ if only one time scale is present [25]. A plot of $L^{\beta/\nu_\perp} \rho_a(t)$ versus t/L^z yields a data collapse to a scaling function that is independent of L. In the present case (Fig. 9), we see that the collapse is imperfect and that the form of $\rho_a(t)$ changes with L. Here z was chosen so as to optimize the collapse at long times, yielding $z = 1.75(3)$. For large systems, the active-site density exhibits three distinct re-

gimes before reaching the quasistationary state: an initial power-law decay (I), followed by a crossover to a slower power-law regime (II), and finally a rapid approach (III) to the stationary state. For $L = 20\,048$, the exponents associated with regimes I and II are 0.163 and 0.144, respectively. While the latter exponent is in reasonable agreement with the scaling relation $\beta_W + \theta = 1$, it is clear that relaxation to the stationary state is more complicated for the sandpile than for, say, the contact process, which presents a unique power-law regime. A qualitative explanation may be found in the interface representation: the short-time dynamics is dominated by relaxation of the initial configuration, which in the interface language means that at short times, columnar noise dominates.

A related facet of the relaxation process is the approach of the mean height to its global value ζ at a site with initial
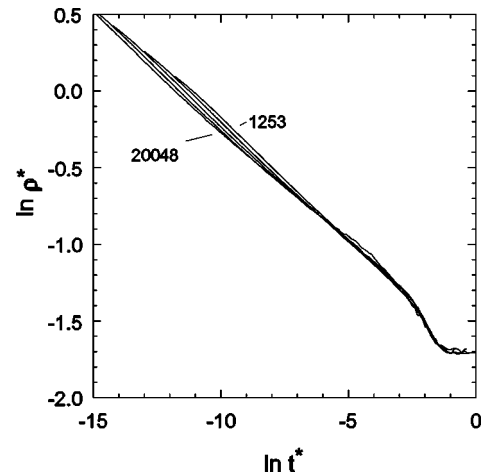

FIG. 9. Scaled active-site density vs scaled time for $\zeta = 0.9489$, system sizes $L = 1253, \ldots, 20\,048$ as indicated.
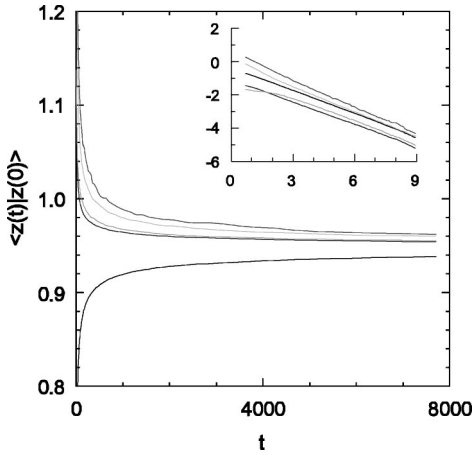
FIG. 10. Mean height $\langle z(t)|z(0)\rangle$ of sites with initial height $z(0)$, in a system of 1400 sites at ζ_c, averaged over 2000 trials. From bottom to top: $z(0) = 0, 1, 2, 3,$ and 4. The inset is a plot of $\ln|\langle z(t)|z(0)\rangle - \zeta|$ vs $\ln t$.

height $z(0)$. In Fig. 10 we plot the mean height $\langle z(t)|z(0)\rangle$ in at system of 1400 sites at ζ_c, averaged over 2000 trials. The inset shows that the asymptotic approach to ζ is approximately power law, $|\langle z(t)|z(0)\rangle - \zeta| \sim t^{-\phi}$, with $\phi \simeq 0.46$, 0.45, 0.47, 0.50, and 0.53 for $z(0) = 0, 1, 2, 3,$ and 4, respectively. All of these exponents are close to $\phi = 1/2$, the value expected for uncorrelated diffusion.

IV. DISCUSSION

We studied the scaling behavior of a one-dimensional fixed-energy sandpile with the same local dynamics as the Manna model. The model exhibits a continuous phase transition between an absorbing state and an active one at a critical particle density $\zeta_c = 0.948\,85(7)$. The phase transition in the one-dimensional stochastic sandpile is characterized by the critical exponents $\beta = 0.42(2)$ and $\nu_\perp = 1.81(1)$, which differ significantly from those associated with directed percolation ($\beta = 0.2765, \nu_\perp = 1.0968$) and linear-interface depinning [$\beta = 0.25(3), \nu_\perp \simeq 1.3$]. While absorbing-state phase transitions are expected to fall generically in the directed percolation universality class [27,28], it is reasonable to exempt the Manna model from this rule due to local conservation of particles; this conservation law is expected to alter the universality class. In fact, studies of various models with the same local conservation law as the Manna sandpile, in dimensions $d > 1$, indicate a common universality class for models sharing this feature [12,14,29].

Studying the interface representation of the model, we obtain the roughness exponent $\alpha = 1.48(2)$ and growth exponent $\beta_W = 0.86(2)$, which should be compared with $\alpha = 1.33(1)$, $\beta_W = 0.839(1)$ for DP and $\alpha = 1.25(1)$, $\beta_W = 0.88(2)$ for LIM. Study of the height-height correlation function yields the local roughness exponent $\alpha_{loc} = 0.59(3)$; the corresponding DP value is $0.63(3)$ [25].

Given the discrepancy between sandpile and LIM exponents found here, the apparent agreement between these sets of exponents in two dimensions suggests that either the numerical equivalence is fortuitous, or that the noise in the interface equation has a fundamentally different structure depending on the dimension. It is worth remarking that our result for roughness exponent is rather close to $\alpha = 3/2$, the value one expects if only the columnar component of the noise is relevant [30]. The other exponents, however, seem to be far from the columnar-disorder universality class (i.e., $\nu_\perp = 2$, $z = 2$, $\beta = 1$, and $\beta_w = 3/4$) [30]. In linear interface models, translational invariance of the noise can be used to derive the scaling relation $(2-\alpha)\nu_\perp = 1$ [31]. Our results do not satisfy this relation.

We determined the dynamic exponent z using several different approaches: (1) scaling of the lifetime at the critical point [$z = 1.63(7)$]; (2) from the temporal rescaling required for a data collapse of the interface width, $W^2(t)$ [$z = 1.65$–1.70]; (3) from a data-collapse analysis of the initial decay of the activity [$z = 1.70(5)$]. Pooling these results we have $z = 1.66(7)$, which rules out the LIM value of $z = 1.42(3)$ [18]. In the context of interface depinning z can be linked to the other exponents via the scaling relation $z = \beta/\nu_\perp + \alpha$ [31]. Inserting the values of β, $\nu_\perp$, and α measured in our simulations, we obtain $z = 1.7$, consistent with our result for z.

We note that the present model does not exhibit the strong nonergodic effects observed in the fixed-energy version of the BTW sandpile. The relaxation of the mean height $\langle z_i(t)\rangle$ from its initial value to the average, ζ, follows a power law with an exponent $\approx 1/2$. We find good evidence for finite-size scaling, in contrast with most driven sandpiles [32–34]. In summary, we have identified a one-dimensional sandpile model that exhibits an absorbing-state phase transition as the relevant temperaturelike parameter (the energy density) is varied. It appears to be the ''minimal model'' for absorbing-state phase transitions belonging to a recently identified universality class associated with a conserved density. Preliminary studies indicate that the driven version of the model exhibits scale-invariant avalanche statistics [3,35]. We may therefore hope that analysis of the driven model, and of spreading of activity at the critical point of the fixed-energy system, will permit us to establish detailed connections between scale invariance under driving and the underlying absorbing-state phase transition.

Let us stress, finally, that while in higher dimensions the linear-interface depinning universality class appears to coincide with that of an absorbing-state phase transition in the presence of a conserved static field, our present results show that this equivalence is violated in $d = 1$. It will be interesting to study other one-dimensional systems with absorbing states and an order parameter coupled to a static conserved field [4,14,29] in order to compare the critical exponents and anomalies with those reported in this paper.

[1] P. Bak, C. Tang, and K. Wiesenfeld, Phys. Rev. Lett. **59**, 381 (1987); Phys. Rev. A **38**, 364 (1988).

[2] G. Grinstein, in *Scale Invariance, Interfaces and Nonequilibrium Dynamics*, Vol. 344 of *NATO Advanced Study Institute, Series B: Physics*, edited by A. McKane *et al*. (Plenum, New York, 1995).

[3] R. Dickman, M.A. Muñoz, A. Vespignani, and S. Zapperi, Braz. J. Phys. **30**, 27 (2000); cond-mat/9910454.

[4] M. A. Muñoz, R. Dickman, R. Pastor-Satorras, A. Vespignani, and S. Zapperi, in *Procedings of the Sixth Granada Seminar on Computational Physics*, edited by J. Marro and P. L. Garrido (AIP, New York, 2001).

[5] C. Tang and P. Bak, Phys. Rev. Lett. **60**, 2347 (1988).

[6] A. Vespignani and S. Zapperi, Phys. Rev. Lett. **78**, 4793 (1997); Phys. Rev. E **57**, 6345 (1998).

[7] R. Dickman, A. Vespignani, and S. Zapperi, Phys. Rev. E **57**, 5095 (1998).

[8] A. Vespignani, R. Dickman, M.A. Muñoz, and Stefano Zapperi, Phys. Rev. Lett. **81**, 5676 (1998).

[9] M.A. Muñoz, R. Dickman, A. Vespignani, and Stefano Zapperi, Phys. Rev. E **59**, 6175 (1999).

[10] A. Chessa, E. Marinari, and A Vespignani, Phys. Rev. Lett. **80**, 4217 (1998).

[11] A. Montakhab and J.M. Carlson, Phys. Rev. E **58**, 5608 (1998).

[12] A. Vespignani, R. Dickman, M.A. Muñoz, and S. Zapperi, Phys. Rev. E **62**, 4564 (2000).

[13] M. Alava and K.B. Lauritsen, Europhys. Lett. **53**, 569 (2001); e-print cond-mat/0002406.

[14] M. Rossi, R. Pastor-Satorras, and A. Vespignani, Phys. Rev. Lett. **85**, 1803 (2000).

[15] D. Dhar, Physica A **263**, 4 (1999), and references therein.

[16] V.B. Priezzhev, J. Stat. Phys. **74**, 955 (1994); E.V. Ivashkevich, J. Phys. A **27**, 3643 (1994); E.V. Ivashkevich, D.V. Ktitarev and V.B. Priezzhev, Physica A **209**, 347 (1994).

[17] J. Marro and R. Dickman, *Nonequilibrium Phase Transitions in Lattice Models* (Cambridge University Press, Cambridge, 1999).

[18] H. Leschhorn, Physica A **195**, 324 (1993).

[19] M. Paczuski, S. Maslov, and P. Bak, Europhys. Lett. **27**, 97 (1994); **28**, 295 (1994).

[20] S.S. Manna, J. Phys. A **24**, L363 (1991).

[21] S.S. Manna, J. Stat. Phys. **59**, 509 (1990).

[22] M. E. Fisher, in *Fenomini Critici*, Proceedings of the International School of Physics ''Enrico Fermi,'' Course LI, Varenna, 1970 (Academic Press, New York, 1971); M.E. Fisher and M.N. Barber, Phys. Rev. Lett. **28**, 1516 (1972); *Finite Size Scaling*, edited by J. Cardy, (North-Holland, Amsterdam, 1988).

[23] A.-L. Barabási and H. E. Stanley, *Fractal Concepts in Surface Growth* (Cambridge University Press, Cambridge, 1995).

[24] T. Halpin-Healy and Y.-C. Zhang, Phys. Rep. **254**, 215 (1995).

[25] R. Dickman and M.A. Muñoz, Phys. Rev. E **62**, 7632 (2000).

[26] J.M. López, M.A. Rodríguez, and R. Cuerno, Phys. Rev. E **56**, 3993 (1997); J.M. López, Phys. Rev. Lett. **83**, 4594 (1999).

[27] H.K. Janssen, Z. Phys. B: Condens. Matter **42**, 141 (1981); **58**, 311 (1985).

[28] P. Grassberger, Z. Phys. B: Condens. Matter **47**, 465 (1982).

[29] R. Pastor-Satorras and A. Vespignani, Phys. Rev. E **62**, R5875 (2000).

[30] G. Parisi and L. Pietronero, Europhys. Lett. **16**, 321 (1991); Physica A **79**, 16 (1991).

[31] M. Kardar, Phys. Rep. **301**, 85 (1998).

[32] L.P. Kadanoff, S.R. Nagel, L. Wu, and S. Zhou, Phys. Rev. A **39**, 6524 (1989).

[33] M. De Menech, A.L. Stella, and C. Tebaldi, Phys. Rev. E **58**, R2677 (1998); C. Tebaldi, M. De Menech, and A.L. Stella, Phys. Rev. Lett. **83**, 3952 (1999).

[34] B. Drossel, Phys. Rev. E **61**, R2168 (2000).

[35] R. Dickman (unpublished).